High-bandwidth viscoelastic properties of aging colloidal glasses and gels

S. Jabbari-Farouji,[1,2] M. Atakhorrami,[3] D. Mizuno,[3,4,5] E. Eiser,[6,7] G. H. Wegdam,[1] F. C. MacKintosh,[3]
Daniel Bonn,[1,8] and C. F. Schmidt[4,5]

[1]*van der Waals-Zeeman Institut, Universiteit van Amsterdam, 1018XE Amsterdam, The Netherlands*

[2]*Theoretical and Polymer Physics Group, Department of Applied Physics, Technische Universiteit Eindhoven,
5600 MB Eindhoven, The Netherlands*

[3]*Department of Physics and Astronomy, Vrije Universiteit Amsterdam, 1081HV Amsterdam, The Netherlands*

[4]*Organization for the Promotion of Advanced Research, Kyushu University, Higashi-ku, Hakozaki 6-10-1, 812-0054 Fukuoka, Japan*

[5]*3. Physikalisches Institut, Georg-August-Universität, 37077 Göttingen, Germany*

[6]*van 't Hoff Institute for Molecular Sciences, Universiteit van Amsterdam, 1018WV Amsterdam, The Netherlands*

[7]*University of Cambridge, Department of Physics, Cavendish Laboratory, J J Thomson Avenue,
Cambridge CB3 0HE, United Kingdom*

[8]*Laboratoire de Physique Statistique de l'ENS, 75231 Paris Cedex 05, France*

We report measurements of the frequency-dependent shear moduli of aging colloidal systems that evolve from a purely low-viscosity liquid to a predominantly elastic glass or gel. Using microrheology, we measure the local complex shear modulus $G^*(\omega)$ over a very wide range of frequencies (from 1 Hz to 100 kHz). The combined use of one- and two-particle microrheology allows us to differentiate between colloidal glasses and gels—the glass is homogenous, whereas the colloidal gel shows a considerable degree of heterogeneity on length scales larger than 0.5 μm. Despite this characteristic difference, both systems exhibit similar rheological behaviors which evolve in time with aging, showing a crossover from a single-power-law frequency dependence of the viscoelastic modulus to a sum of two power laws. The crossover occurs at a time t_0, which defines a mechanical transition point. We found that the data acquired during the aging of different samples can be collapsed onto a single master curve by scaling the aging time with t_0. This raises questions about the prior interpretation of two power laws in terms of a superposition of an elastic network embedded in a viscoelastic background.

I. INTRODUCTION

Soft glassy materials are ubiquitous in everyday life. A common feature of all such materials is their relatively large response to small forces (hence soft) and their disordered (glassy) nature. Pertinent examples of such systems are foams, gels, slurries, concentrated polymer solutions, and colloidal suspensions. These systems show interesting viscoelastic properties; depending on the frequency with which they are perturbed, they can behave either liquid or solid like. In spite of their importance for numerous applications, the mechanical behavior of such soft glassy materials is still not completely understood [1].

In recent decades, colloidal suspensions have been used extensively as model systems for the glass transition in simple liquids [2–4] and gel formation [5], since the diffusion of the particles can easily be measured using, e.g., light scattering or confocal microscopy [6]. The viscoelasticity of such systems, especially its development during the aging of glassy systems or the formation of a gel, has, however, received relatively little attention.

Another issue that deserves attention is differentiating between colloidal gels and glasses in terms of their rheological properties [7]. The main difference between colloidal gels and glasses stems from their spatial structure [4]. Colloidal glasses can be defined as systems with a liquidlike structure having no long-range order. Just as liquids, glassy systems have a homogenous spatial structure, as, for instance, evi-

denced by the structure factor measured by scattering experiments [4]. On the other hand, a colloidal gel can be defined as a system in which attractive interactions play an important role, leading to a structure that is heterogeneous on a length scale much larger than the particles. This may be due either to the formation of clusters of particles or a system-spanning network, leading to a q-dependent structure factor. The difference between glassy and gel systems in the system we study here is clear from the scattering experiments shown in Fig. 1 [8]. We emphasize here that we talk about spatial heterogeneities in the structure of the gel and glassy phases, which should be distinguished from dynamic heterogeneity sometimes observed in glasses [6]. Detecting dynamic heterogeneity requires the measurements of four-point spatiotemporal correlations which is beyond the scope of this paper [9]. In addition to the structural differences, the different character of gels and glasses leads to different aging behavior for these systems, for example, when the diffusion of particles is measured as a function of aging time, which is coinsidered elsewhere [8,10]; here, we focus on the viscoelastic properties.

We focus on the viscoelasticity of clay Laponite suspensions for which a rich phase diagram has been reported [11,12]. When dissolved in water, Laponite suspensions evolve from a liquidlike state to a nonergodic solidlike state [3,4,13,14]. During this process the mobility of the particles slows down and viscoelasticity develops. This system is an interesting one to study, since both colloidal gels and glasses
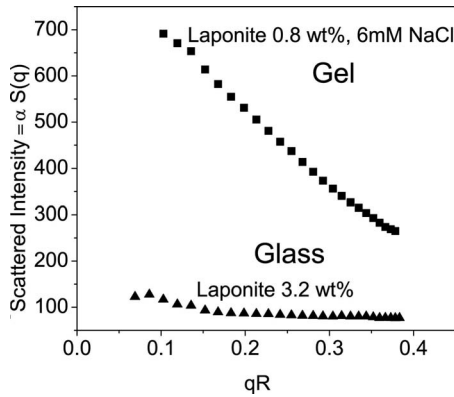
FIG. 1. Light scattering-intensity reduced with respect to scattered intensity from toluene for two samples: (a) 3.2 wt % Laponite and (b) 0.8 wt % Laponite, 6 mM NaCl. The data points are taken at late stages of aging when the scattering intensity has stabilized.

can be obtained depending on the Laponite concentration and added salt content; see again Fig. 1 and Ref. [8]. Therefore, it provides us with the possibility to investigate the similarities and differences in the viscoelastic properties of the two types of nonequilibrium states.

To study the mechanical properties of gels and glasses, we used microrheology (MR), which allows us to measure frequency-dependent shear moduli over a wide range of frequencies. This technique is based on the detection of small displacements of probe particles embedded in soft glassy material, from which we obtain the mechanical properties of surrounding matrix [15]. Considering the fragility of soft materials, this technique is ideally suited for our studies, since it is less invasive than conventional rheometry.

Here we have used a combination of one and two-particle MR measurements [16,17] to probe the mechanical properties and possible inhomogeneities of colloidal gels and glasses on length scales of the order of the particle size 1 μm and separation distances of the order of $5-20$ μm.

II. EXPERIMENT

A. Materials

We have studied charged colloidal disks of Laponite XLG, with an average radius of 15 nm and a thickness of 1 nm. Laponite can absorb water, increasing its weight up to 20%. Therefore, we first dried it in an oven at 100 °C for 1 week and subsequently stored it in a desiccator.

We prepared a number of Laponite samples with different concentrations and salt contents. Laponite solutions without added salt were prepared in ultrapure Millipore water (18.2 MΩ cm^{-1}) and were stirred vigorously with a magnet for 1.5 h to make sure that the Laponite particles were fully dispersed. The dispersions were filtered using Millipore Millex AA 0.8-μm filter units to obtain a reproducible initial state [4]. This instant defined the zero of the waiting time, $t_w = 0$.

The Laponite solutions with pH=10 were obtained by mixing the Laponite with a 10^{-4} mole/l solution of NaOH in Millipore water. The samples with nonzero salt content were

prepared by diluting the Laponite suspensions in pure water with a more concentrated salt solution [18]. For instance, a sample of 0.8 wt %, 6 mM NaCl was prepared by mixing equal volumes of 1.6 wt % Laponite solution in pure water with a 12-mM salt solution.

For the microrheology measurements, we added a small fraction, below 10^{-4} vol %, of silica beads with a diameter of 1.16 μm $\pm 5\%$ [19] immediately after the preparation of the sample. Subsequently we infused the solution into a sample chamber of about 50 μl volume, consisting of a coverslip and a microscope slide separated by spacers of double-sided tape with a thickness of 70 μm, sealed with vacuum grease at the ends to avoid evaporation of the sample. All the experiments were performed at room temperature (21 ± 1 °C). After placing the sample chamber into the microscope, we trapped two beads and moved them to about 20 μm above the bottom glass surface.

B. Microrheology

The experimental setup for performing one- and two-particle MR consists of two optical tweezers formed by two independent, polarized laser beams $\lambda_1 = 1064$ nm (Nd:YVO4, cw) and $\lambda_2 = 830$ nm (diode laser, cw) which can trap two particles at a variable separation r. Details of the experimental setup can be found in [16,20]. Stable trapping is achieved using a high-numerical-aperture (high-NA) objective lens which is part of a custom-built inverted microscope. Two lenses in a telescope configuration allow us to control the position of the beam foci in the plane perpendicular to the beam directions. The two beams are focused into the sample chamber through a high numerical objective of the microscope ($100\times$, NA 1.3).

Back-focal-plane interferometry is used to measure the position fluctuations of the probe bead away from the trap center [21]. The signals emerging from each of the traps are separately projected onto two independent quadrant photodiodes, yielding a spatial resolution for the particle position that is better than 1 nm.

During our measurements, the power of each laser was typically less than 10 mW. Labview software was used to acquire time series data of particle positions from the quadrant photo diode for a minimum time of 45 s. The data were digitized with an analog-to-digital (A/D) converter at a 195 kHz sampling rate.

C. Macrorheology

The viscoelastic moduli during the aging process were also measured using a conventional Anton Paar Physica MCR300 rheometer in Couette geometry. To avoid perturbing the sample during the aging process, we performed the oscillatory shear measurements with a strain amplitude of 0.01 in the frequency range of $0.1-10$ Hz. In order to prevent evaporation during the long-time measurements, we installed a vapor trap.

D. Light scattering

Our light-scattering setup (ALV) is based on a He-Ne laser ($\lambda = 632.8$ nm, 35 mW) and avalanche photodiodes as de-

tectors. (Static light-scattering experiments were performed at scattering angle range 20°–150° on nonergodic samples at late stages of aging when the scattered intensity had stabilized. Samples were rotated to average over different positions in the sample.

III. THEORY AND DATA ANALYSIS

There are two classes of MR techniques: active (AMR) and passive (PMR) [22]. In the first of these, the response of a probe particle to a calibrated force is measured. In the second approach, only passive, thermal fluctuations are monitored, from which one can infer the response function and the rheological properties of the surrounding medium using the fluctuation-dissipation theorem (FDT). Applying the FDT assumes thermal equilibrium. It may therefore be potentially problematic to apply PMR to nonequilibrium systems such as aging glasses. Nevertheless, in prior studies [23], we not only directly confirmed the validity of the FDT, but also found excellent agreement between active and passive methods in slowly aging Laponite glass and gel. Therefore, in what follows we will use only the passive method, which has the significant advantage that, with a single measurement of the fluctuation power spectrum, one can determine the complex shear modulus simultaneously over a wide range of frequencies [15,24–26].

A. One-particle microrheology

In one-particle MR, we first extract the complex compliance from the position fluctuations of one particle. The time-series data of the bead displacement measured by the quadrant photodiode are Fourier transformed to calculate the power spectral density of displacement fluctuations:

$$\langle |x(\omega)|^2 \rangle = \int_{-\infty}^{\infty} \langle x(t)x(0) \rangle e^{i\omega t} dt. \tag{1}$$

This is done for x and y directions in the plane normal to the laser beam. The power spectral density of the thermal fluctuations of the probe is related to the imaginary part of the complex compliance $\alpha(\omega) = \alpha'(\omega) + i\alpha''(\omega)$ via the FDT:

$$\alpha''(\omega) = \frac{\omega \langle |x(\omega)|^2 \rangle}{2k_B T}. \tag{2}$$

Provided that $\alpha''(\omega)$ is known over a large enough range of frequencies, one can recover the real part of the response function from a Kramers-Kronig (principal value) integral:

$$\alpha'(\omega) = \frac{2}{\pi} P \int_0^{\infty} \frac{\omega' \alpha''(\omega')}{\omega'^2 - \omega^2} d\omega'. \tag{3}$$

Before calculating the shear modulus from the response function, we calibrate the setup and correct for the trap stiffness that shows up at low frequencies as explained in detail in [17,21].

The complex shear modulus $G^*(\omega) = G'(\omega) - iG''(\omega)$ can be obtained from the corrected complex compliance through the generalized Stokes relation, valid for incompressible and homogenous viscoelastic materials [15,24]:

$$G^*(\omega) = \frac{1}{6\pi R \alpha(\omega)}, \tag{4}$$

where R is the radius of the probe bead.

B. Two-particle microrheology

In two-particle MR, we calculate the correlated fluctuations of two probe beads inside the material. Such measurements probe the viscoelastic properties of the medium on length scales comparable to the interparticle separation. In general, with more than one probe particle, the displacement of particle m in direction i is related to the force applied to particle n in direction j via the complex response tensor $u_i^{(m)}(\omega) = \alpha_{ij}^{(m,n)}(\omega) F_j^{(n)}(\omega)$. In the case of two particles, the response tensors $\alpha_{ij}^{(1,1)}$ and $\alpha_{ij}^{(2,2)}$ describe how each of particles 1 and 2 responds to the forces applied to the particle itself, while $\alpha_{ij}^{(1,2)}$ describes how particle 1 responds to the forces on particle 2.

In thermal equilibrium and in the absence of external forces, the FDT again relates the imaginary part of the response tensor to the spectrum of displacement fluctuations of the particles:

$$\alpha_{ij}^{(m,n)}(\omega) = \frac{\omega}{2k_B T} S_{ij}^{(m,n)}(\omega), \tag{5}$$

where the spectra of thermal fluctuations $S_{ij}^{(m,n)}$ are defined as

$$S_{ij}^{(m,n)}(\omega) = \int_{-\infty}^{\infty} \langle u_i^{(m)}(t) u_j^{(n)}(0) \rangle e^{i\omega t} dt. \tag{6}$$

The problem of two hydrodynamically correlated particles in a viscoelastic medium and the relation between the response tensor and the rheological properties of the medium have been worked out in [27]. The self-parts of the response tensor $\alpha_{ii}^{(1,2)}$ are the same as the ones obtained from one-particle microrheology.

The cross-component part of the response tensor $\alpha_{ij}^{(1,2)}$ can be decomposed into two parts $\alpha_{\parallel}$ parallel to the vector **r** separating the two beads and $\alpha_{\perp}$ perpendicular to **r**: $\alpha_{ij}^{(1,2)} = \alpha_{\parallel} \hat{r}_i \hat{r}_j + \alpha_{\perp}(\delta_{ij} - \hat{r}_i \hat{r}_j)$. For incompressible fluids each of the components is related to the complex shear modulus via a generalization of the Oseen tensor:

$$\alpha_{\parallel}(\omega) = 2\alpha_{\perp}(\omega) = \frac{1}{4\pi r G^*(\omega)}. \tag{7}$$

Similarly to the one-particle method, the measured response function must be corrected for the trap stiffness. The trap correction for two-particle microrheology has been explained in detail in Ref. [17].

IV. RESULTS

We carried out the measurements on a variety of Laponite concentrations and salt contents (2.8, 3.2 wt %, in pure water, 3 wt % in pH=10, 1.5 wt %, 5 mM NaCl, 0.8 wt %, 6 mM NaCl, 0.8 wt %, 3 mM NaCl). We have chosen these samples to ensure that their rate of aging is slow enough to guarantee that no significant aging occurs during each mea-
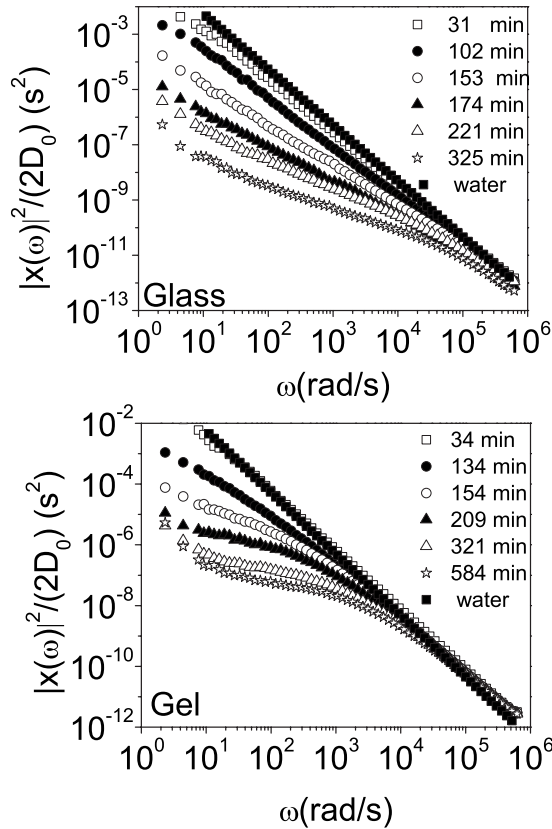
FIG. 2. Normalized displacement power spectral densities $\langle |x(\omega)|^2 \rangle / 2D_0$ of silica probe particles in a glassy sample (3.2 wt %, bead diameter 1.16 μm) and a gel-like sample (0.8 wt %, 6 mM NaCl, bead diameter 0.5 μm) in the x direction with increasing age after preparing the sample. Aging times are given in the legend. The solid squares show the PSD of a bead in pure water for comparison. All experiments were done at 21 °C.

surement. On the other hand, they evolve fast enough to allow us to follow the whole evolution within a few hours. The samples 2.8 and 3.2 wt %, in pure water, 3 wt % in pH=10, and 1.5 wt %, 5 mM NaCl showed the properties of a glassy sample according to our light-scattering data, and samples 0.8 wt %, 6 mM NaCl, 0.8 wt %, 3 mM NaCl behaved like a colloidal gel [10,28]. In addition, we find that a pH of 10 did not affect the aging dynamics qualitatively. It merely acted as an electrolyte that slightly accelerated the aging. The same held for Laponite 1.5 wt %, 5 mM NaCl. In this case salt just accelerated the aging, but it did not change the underlying dynamics of the aging process and the structure remained homogeneous.

For a detailed discussion of our results, we focus on two samples that are representative of the others: one sample that behaves as a glass (C=3.2 wt %) and one sample (C=0.8 wt %, 6 mM NaCl) that behaves like a gel. In the latter case, the structure factor shows a strong q dependence, as illustrated in Fig. 1. This suggests a more heterogenous, gel-like structure, in contrast to the more homogenous samples that we identify as a glass. In the following, we shall characterize our samples as gels or glasses in this way.

To follow the aging of the systems we trapped a bead in a single laser trap and measured the displacement power spec-

tral densities (PSD) as a function of waiting time. Since the system evolves towards a nonergodic state, the time average may not necessarily be equal to the ensemble average for the measured PSDs. However, in our range of frequencies $(1-10^5$ Hz$)$ we confirmed that our results did not depend on the time interval used to compute the time average. Thus, we can use the time-averaged PSD without averaging over several beads in our study.

Figure 2 shows the measured displacement PSDs as a function of frequency during the aging of the glass and the gel, respectively. We normalized the PSDs with the diffusion coefficient $D_0 = kT/(6\pi \eta_{water} R_{bead})$ of a same-size bead measured in water, so that the normalized PSDs will be independent of bead size. It is evident that in both systems the particle motion progressively slows down with increasing aging time t_a, reflecting the increase of viscosity in the system. The PSDs in both samples start from a state close to water, for which $\langle |x(\omega)|^2 \rangle / 2D_0 = 1/\omega^2$. Gradually their amplitudes as well as the absolute values of their power-law slopes decrease with time. There is a crossover time t_0 such that for $t_a < t_0$, the PSDs can be described by a single power law. At longer aging times $t_a > t_0$, two distinct slopes appear in the log-log plots (Fig. 2).

The evolution of the local shear moduli G^* obtained from PSDs is shown in Fig. 3 (glass) and Fig. 4 (gel). The shear moduli are derived from single particle MR according to Eq. (4). It is evident that the systems evolve from an initially completely viscous to a strongly viscoelastic fluid. At the early stages of aging, the loss modulus is still much larger than the storage modulus ($G'' \gg G'$), representing a more liquidlike state. With time the samples become more solid like: the elastic modulus becomes larger than the loss modulus ($G'' \ll G'$). We observe also that the changes in G' are more dramatic than the changes in G''. While G'' almost saturated after 170 min for the glass and 100 min for the gel, G' continues to grow with time.

Inspection of the different samples reveals that the gel is "softer" than the glass. When we mechanically shook similar tubes containing gel or glass, the gel liquefied at a clearly smaller stress: it appears that gels had a lower yield stress compared to glasses. Therefore it is reasonable to expect that the gels also have a lower viscoelastic modulus than glasses, as comparison of Figs. 3 and 4 indeed confirms. However, one should note that the gels studied here are at a smaller concentration of Laponite, so that we are not able to compare the gel and glass of the same concentration.

From microrheology we conclude that the aging behaviors of gels and glasses are qualitatively similar. We know, however, from light scattering measurements that the underlying structures of gels and glasses are very different [8]. Since spatial heterogeneity is the defining feature of gels, we thus set out to investigate if local measurements of microrheology across the samples can detect the difference between gels and glasses.

A. Heterogeneity

Heterogeneities within a sample can be explored by measuring the PSDs of multiple beads at different positions in
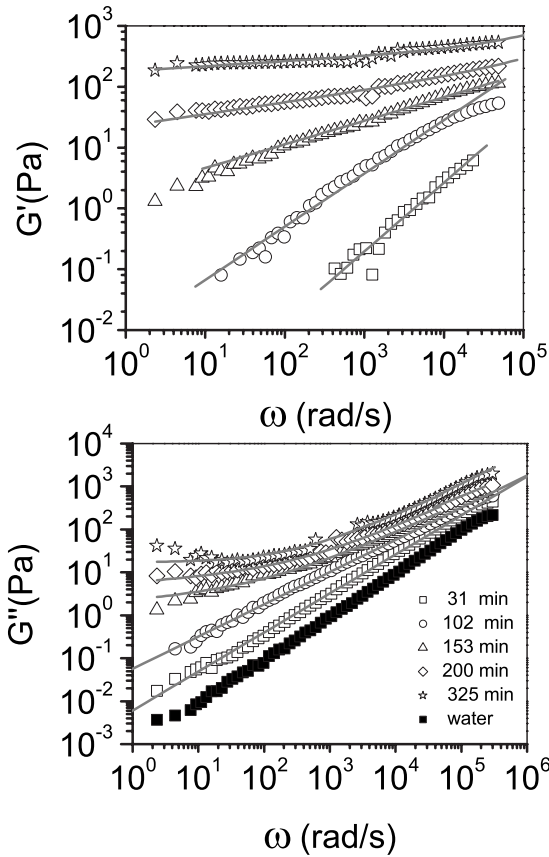
FIG. 3. Glass data: the symbols show the shear moduli $G'(\omega)$ and $G''(\omega)$ (absolute magnitude) as a function of frequency measured using 1.16-μm silica probe particles in a 3.2 wt % Laponite solution in pure water with increasing aging time after preparing the sample. Aging times are given in the legend. The lines show the fits of $G'(\omega)$ and $G''(\omega)$ according to $C_1(-i\omega)^a + C_2(-i\omega)^b$ in which $C_2 = 0$ for aging times $t_a < 120$ min.

the sample. A discrepancy between the shear moduli obtained from one- and two-particle MR can also be used as an indicator of a heterogeneous structure. A further test of heterogeneity in a material is provided by comparison of MR with bulk rheology, as will be discussed below. To investigate the homogeneity of colloidal gels and glasses of Laponite, we performed two types of measurement. First, we made simultaneous measurements of PSDs of two independent beads in two independent traps at different stages of aging. In another set of experiments, we measured PSDs of multiple beads in aged gels and glasses. The results of our experiments for both gels and glasses will be discussed below.

1. Glass

For the glassy samples the displacement PSDs turned out to be independent of the bead position, as was concluded from a comparison of simultaneous measurements of PSDs of two independent beads in two independent traps during aging. Furthermore, the comparison between one- and two-particle MR reveals that within the experimental error, the complex shear moduli are identical to within the experimen-
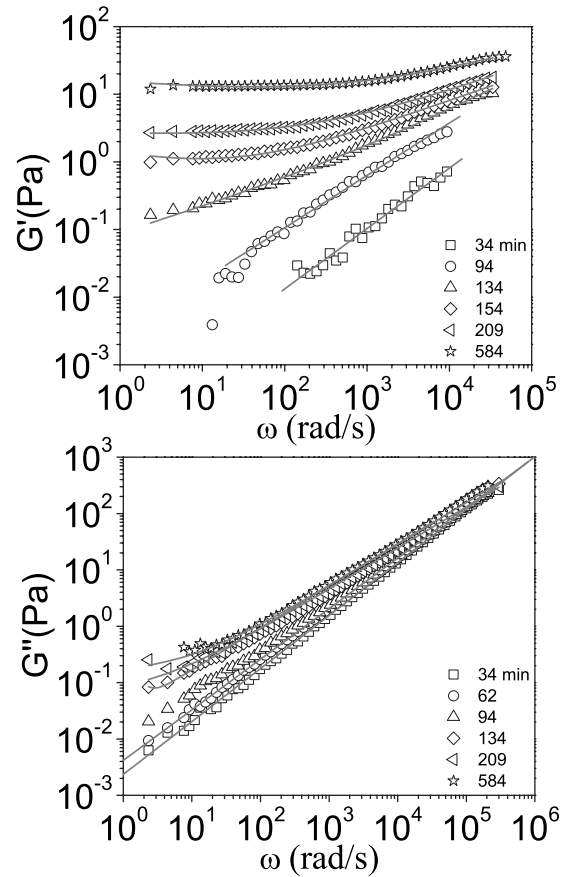

FIG. 4. Gel data: the symbols show the shear moduli $G'(\omega)$ and $G''(\omega)$ (absolute magnitude) as a function of frequency measured using a 0.5-μm silica probe particle in a 0.8 wt % Laponite solution in 6 mM NaCl water with increasing aging time after preparing the sample. Aging times are given in the legend. The lines show the fits of $G'(\omega)$ and $G''(\omega)$ according to $C_1(-i\omega)^a + C_2(-i\omega)^b$ in which $C_2 = 0$ for aging times $t_a < 100$ min.

tal error between the two methods for all stages of aging as shown in Fig. 5.

This was further verified by measuring the PSDs of several beads at different positions of an aged sample. As can be seen in Fig. 6, the measured shear moduli were independent of the position of the bead in the sample, verifying the homogeneity of the glassy sample, as shown also in Fig. 7(a).

These results suggest that the Laponite glass has a homogenous viscoelasticity, at least on length scales larger than half a micrometer, which is the length scale one-particle MR intrinsically averages over. An additional check on this can be obtained from a comparison between microrheology and macrorheology, which should yield the same results if the sample is homogeneous.

Figure 8 shows the shear moduli extracted from MR and macrorheology experiments at a fixed frequency of ($f = 0.7$ Hz) during the course of aging. The overall agreement between macrorheology and MR is good. For the early stages of aging, the G'' measured by the macrorheometer appears slightly higher, but this can be attributed to the large moment of inertia of the rheometer bob; macrorheology does not provide accurate measurements of the shear moduli when
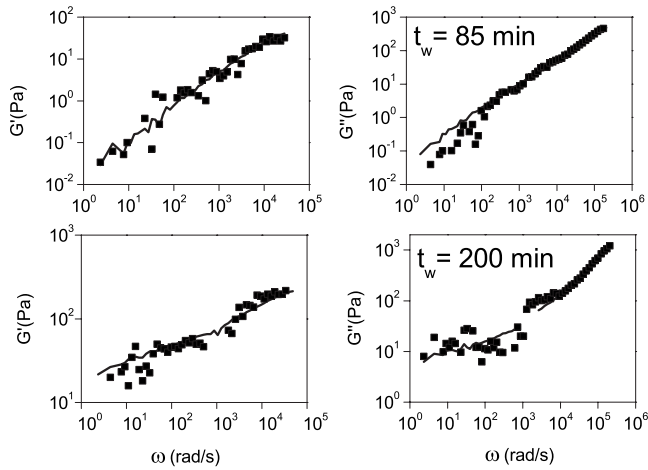
FIG. 5. Glass data: the shear moduli $G'(\omega)$ and $G''(\omega)$ (magnitude) at two different stages of aging in a 3.2 wt % Laponite solution derived from one-particle (lines) and two-particle (symbols) MR using 1.16-μm silica probe particles. The distance between the two particles was 6 μm. The aging times are shown in the figure. Note that in the late stages of aging the material becomes too stiff to obtain a good cross-correlation signal between the two beads over the background noise.

$G^* < 1$ Pa. MR, on the other hand, has other sources of errors at low frequencies, especially for the late stages of aging, when the material becomes very rigid. In this case, the signal detected by the photodiode becomes small compared to the noise level; $1/f$-laser-pointing noise dominates at low frequencies. This is the most plausible explanation for the slight discrepancy between the results from the two methods at long aging times.

2. Gel

Measuring the displacement PSDs of several beads at different positions of a gel at the late stages of aging revealed a considerable degree of inhomogeneity [Fig. 6(b)]. Not only were the PSDs position dependent, but at some positions in the sample the measured PSDs were also anisotropic, i.e., fluctuations in the x and y directions gave different results.

This result is consistent with the static light scattering measurements for this sample shown in Fig. 1 that suggest inhomogeneities of the gel on a length scale comparable to the inverse scattering vector—i.e., micrometers. Therefore, exploring such a gel using microrheology with a probe on the order of the mesh size of the network, one can detect these characteristic inhomogeneities. In Fig. 9 we have plotted the shear moduli seen by the beads at different positions. It can be seen that there was an order-of-magnitude difference between the smallest and largest elastic moduli measured in the same sample and at the same time.

It is intriguing to ask when the heterogeneity starts to develop in the aging samples. It is likely to appear as a networklike structure building up in the gel. To answer this question, we measured the PSDs of two beads at different positions of a gel as a function of aging time. We performed two sets of experiments: in the first one the two beads were positioned at a relatively close distance $r=4.66\ \mu$m (Fig. 10)
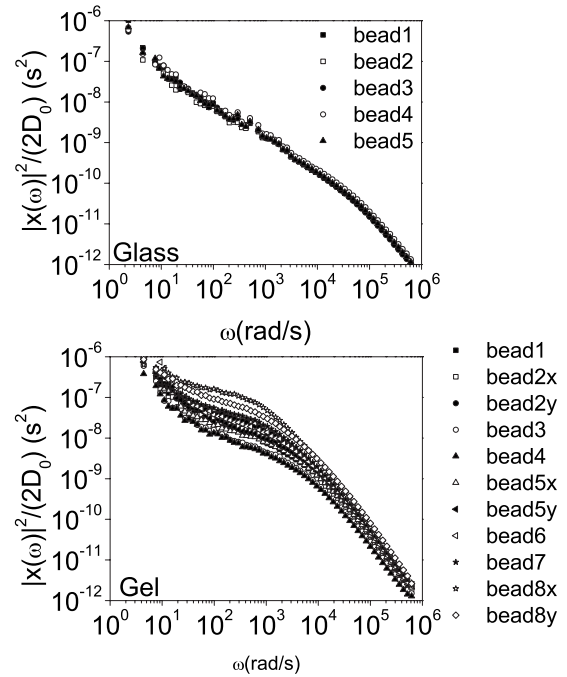

FIG. 6. The displacement PSDs of 0.5-μm silica beads measured at different positions within an aged glass (3.2 wt % Laponite in pure water, $t_w \approx 5$ h) and within an aged colloidal gel (0.8 wt % Laponite in 6 mM NaCl solution, $t_a \approx 10$ h).

and in the other one at a large distance of $r=19\ \mu$m.

In both experiments, the responses—i.e., the PSDs—at different positions were equal in the early stages of aging. However, as time progressed, the PSDs measured at different positions began to differ. In addition, at later stages of aging, the displacement PSDs measured for some of the beads became anisotropic, meaning that the PSDs in the x and y directions were not equal anymore. In some measurements the anisotropy survived the latest measurement. For some other measurements, the anisotropy disappeared after some time (see Fig. 10, for example). This suggests that the building up of structure in the gel is a dynamic process; at some points and times, more particles join the network and at some other points and times some particles disintegrate from the network.

Furthermore, our experiments showed that immediately after preparation, shear moduli obtained from two-particle MR and one-particle MR were equal. But already at relatively early stages of aging, the two-particle MR results differed from one-particle MR results as demonstrated in Fig. 10. This deviation appeared long before the local shear moduli of the two beads in one-particle MR started to differ. For more details, see also [28].

Our measurements on several bead pairs at varying distances suggest that these inhomogeneities extend over a range of at least 100 μm. Therefore the macroscopic bulk shear modulus is not necessarily expected to be equal to that measured by single-particle MR. In Fig. 11, we compare the shear moduli obtained from one- and two-particle MR with the results of macrorheology at late stages of aging ($t_a \approx 8.5$ h) when the changes in the loss and elastic moduli are slow. It is evident that the local shear modulus measured at
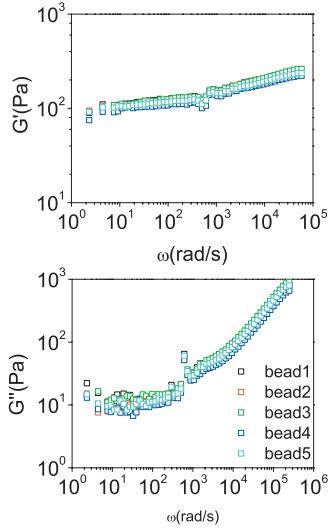
FIG. 7. (Color) Local elastic modulus G' and loss modulus G'' measured at different positions in an aged glassy sample of 3.2 wt % Laponite in pure water ($t_a \approx 5$ h)
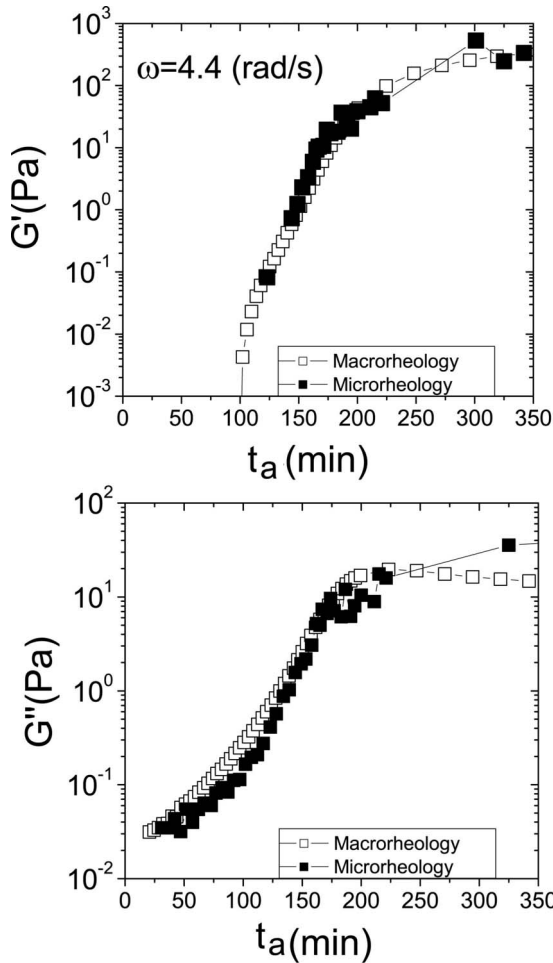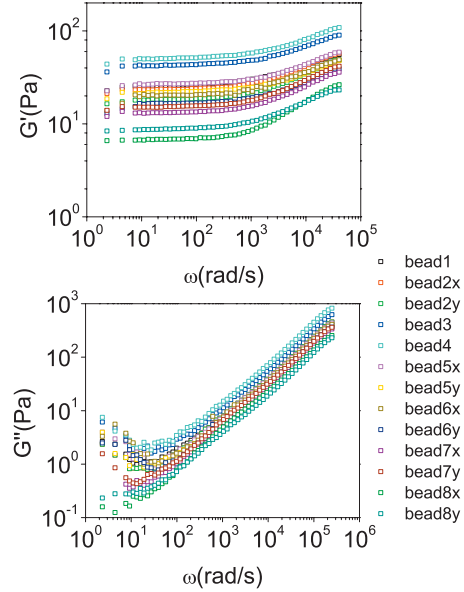

FIG. 9. (Color) Gel data: local elastic modulus G' and loss modulus G'' measured at different positions in an aged gel sample of 0.8 wt % Laponite in 6 mM NaCl solution ($t_a \approx 10$ h).

one of the positions in the sample was equal to the bulk value, while the others reported a considerably lower shear modulus. Notably, the shear modulus obtained from the cross correlation of two-particles is lower than both bulk and local shear moduli. This suggests that two-particle MR can be used to detect inhomogeneities as long as they occur on length scales below the distance between the particles, but the results may still not reflect bulk properties if heterogeneities extend beyond the scale of the interparticle distance.

B. Model for the viscoelastic behavior

It has been noted in the context of weakly attractive colloids [29] and biopolymer networks [30] that the addition of two power-law contributions describes the shear modulus very well. This result appears to reflect the existence of two distinct contributions to the viscoelasticity of the system and can be interpreted as a superposition of a more elastically rigid network (weakly frequency dependent) and viscoelastic background (with a strong frequency dependence).

Our data (Figs. 3 and 4) can be interpreted in a similar manner: In addition to a strongly frequency-dependent viscoelastic response at high frequencies, a more elastic (weakly frequency-dependent) response appears after some aging time t_0 and slowly increases in amplitude during the aging process. To be more precise, we see that the complex shear modulus of both gels and glasses crosses over from a single power law to a superposition of two power laws around a certain waiting time t_0 which depends on the sample ($t_0 \approx 155$ min for the glass sample of 3.2 wt % Laponite and $t_0 \approx 95$ min for the gel sample of 0.8 wt % Laponite, 6 mM NaCl) [23]. The local shear moduli of both samples turn out to be well described by the following expression:

FIG. 8. Elastic and loss modulus as a function of aging time for a sample of 3.2 wt % Laponite in pure water obtained from macrorheology and one-particle MR at $f = 0.7$ Hz. The strain amplitude in the macrorheology measurements was 0.01.
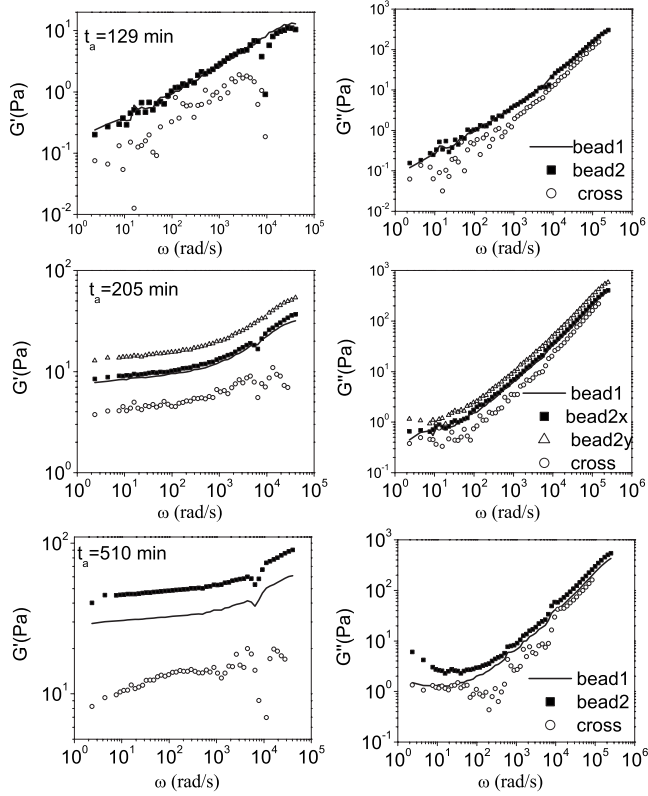
FIG. 11. Complex shear modulus at a late stage of aging $t_a \approx 8.5$ h obtained from single-particle MR at two different positions of the sample, two-particle MR, and bulk rheology in a sample of 0.8 wt % Laponite, 6 mM NaCl. The circles show G' and triangles show G'' values.

We find that the exponent of the single power law decreased from 1 to a value of about 0.7 before the second component becomes visible. The exponent and amplitude of the first component $C_1(-i\omega)^a$ do not change further with aging time for $t_w > t_0$, while the amplitude of the other one C_1 grows appreciably over the same times.

In Figs. 12(a) and 12(c), we have plotted the evolution of the fitting parameters as a function of aging time for different samples. As can be seen in the figure, the development of the two viscoelastic components for different samples is qualitatively similar, although the rate of change depends on sample concentration and salt content.

Interestingly, the evolution curves of the exponents a and b for the different samples superimpose if we scale the aging time as $t_a' = (t_a - t_0)/t_0$. The crossover times are $t_0 = 155$, 95, 120, 105, and 95 min for Laponite concentrations 2.8 wt %, 3 wt %, pH 10, 3.2 wt %, 1.5 wt %, 5 mM, and 0.8 wt %, 6 mM NaCl, respectively. For the amplitudes, on the other hand, the data do not collapse. Especially the amplitudes of the second (viscoelastic) component systematically decrease as the Laponite content is reduced. Furthermore, for the gel the amplitude depends on the position and we can see some fluctuations in the amplitude of the second component C_2, at later stages of evolution. This can be understood in terms of the dynamic process of gel formation in which Laponite particles still can join or detach from the network.

V. DISCUSSION AND CONCLUSION

We have studied the evolution of the viscoelastic properties of a variety of Laponite suspensions including both gel-like and glassy states over a wide range of frequencies using macro- and microrheology techniques. Our measurements reveal the differences between the mechanical properties of gels and glasses.

The glassy samples are homogenous on all length scales probed in our experiments ($l > 0.5$ μm). This is further con-

FIG. 10. Gel data: the shear moduli $G'(\omega)$ and $G''(\omega)$ at different stages of aging derived from one- and two-particle MR of 0.5-μm silica probe particles in a gel of 0.8 wt % Laponite in 6 mM NaCl solution. The distance between the two beads was 4.66 μm. For $t_a = 129$ min the shear moduli at two different positions are equal. At $t_a = 205$ min the shear moduli at the two positions are not equal. Furthermore, shear modulus at position 2 shows anisotropy. At a later time $t_a = 510$ min the shear moduli at the two positions are not equal, but the anisotropy observed earlier at position of bead 2 has disappeared.

$$G^*(\omega) = G'(\omega) - iG''(\omega)$$
$$\equiv \begin{cases} C_1(-i\omega)^a, & t_a < t_0, \\ C_1(-i\omega)^a + C_2(-i\omega)^b, & t_a > t_0. \end{cases} \quad (8)$$

Physically, this model implies that two distinct stresses arise under a common imposed strain—in the way forces add for springs in parallel, as opposed to displacements and compliances that would add for springs in series. This response would be expected, for instance, for two interpenetrating structures and systems that displace together under strain, at least on the scale of our probe particles, which are large compared to the individual Laponite particles. This can, in principle, be the case whether or not the material appears to be homogeneous on this scale. A tenuous elastic network structure immersed in a more fluidlike background, such as we might expect for a gel, would behave in this way, provided that the network and the background medium are strongly coupled hydrodynamically and that the network spans length scales corresponding to the imposed strain. Such a gel could appear to be either homogenous or heterogeneous, depending on the length scale probed.
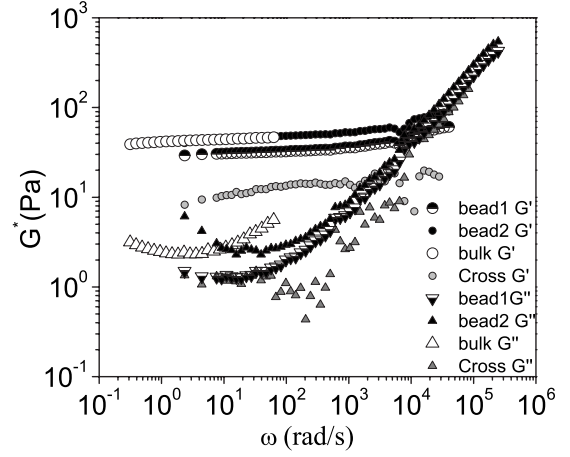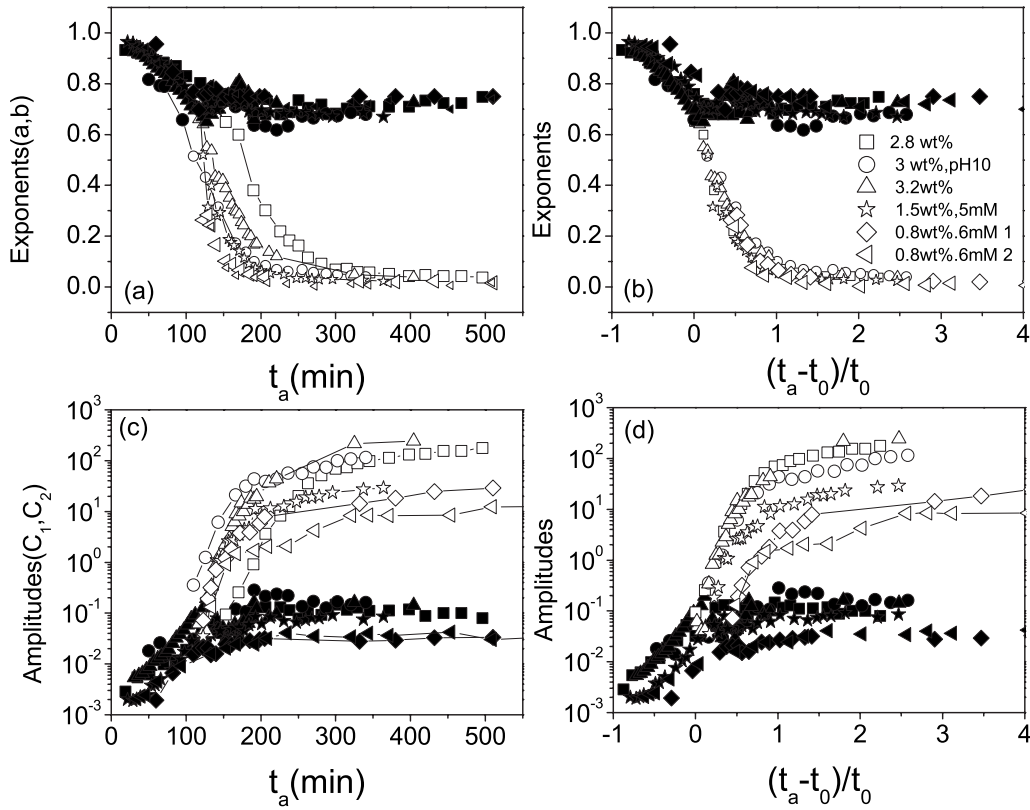
FIG. 12. The complex shear moduli of Laponite suspensions can be described as the sum of two power laws $C_1(-i\omega)^a + C_2(-i\omega)^b$ in which $C_2 = 0$ for waiting times $t_a < t_0$. The crossover times are $t_0 = 155, 95, 120, 105, 95$ min for Laponite concentrations 2.8 wt %, 3 wt %, pH $= 10$, 3.2 wt %, 1.5 wt %, 5 mM NaCl and two different positions of 0.8 wt %, 6 mM NaCl, respectively. (a) The evolution of power-law exponents a (solid symbols) and b (open symbols) as a function of aging time for different concentrations of Laponite. (b) The exponents a (solid symbols) and b (open symbols) as a function of scaled aging time (c) The amplitude of viscoelastic contributions C_1 (solid symbols) and C_2 (open symbols) as a function of aging for different samples. (d) The same as panel (c) but plotted versus scaled aging time. The sample concentrations are shown in the legend.

firmed by comparing microrheology and conventional macrorheology results. We find that measurements at different scales all give the same results. Thus, there is no evidence for spatial inhomogeneity as expected for glassy systems in general.

In the gels, however, along with the evolution from a liquidlike state to a viscoelastic state, inhomogeneities develop in time. These inhomogeneities are detected by measuring the local shear moduli at different positions within the samples at nearly equal waiting times.

When we track the values of the elastic modulus at a fixed frequency (here 0.05 Hz) at late stages of aging, when there is a crossover from a fast aging rate to a slower aging rate, we find that the elastic modulus scales linearly with concentration. One can roughly estimate the plateau value for glasses as $G'_P \propto kT/D^3$, where D is the characteristic structural length of the system. We have taken D as half of the interparticle distance. This estimate predicts the order of magnitude fairly well. From the data shown in Fig. 13, a linear extrapolation suggests that no glassy samples exist at concentrations lower than 1.6 wt %.

Therefore the elasticity for samples with lower concentrations should stem from a different mechanism. Indeed, in such samples the aging proceeds through gel formation. For

comparison, we have shown the elastic modulus of a gel sample of 0.8 wt %, 6 mM in Fig. 13.

Despite the differences between gels and glasses, we find a similar frequency dependence of the viscoelastic moduli
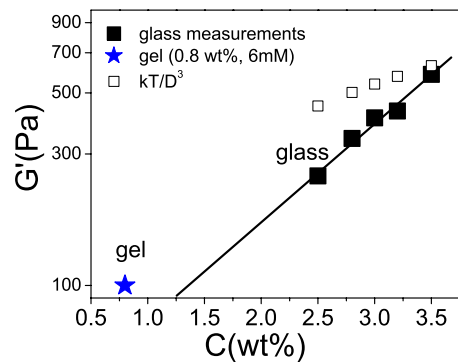
FIG. 13. (Color online) Bold symbols: the elastic modulus obtained from macrorheology at late stages of aging at the aging time that there is a crossover from a fast regime of aging to a slower regime as a function of concentration measured for different glassy samples and a gel sample of 0.8 wt %, with 6 mM salt at $f = 0.05$ Hz. Open symbols: An estimate of the plateau value $G'_P \propto kT/D^3$ is shown for comparison.

for gels and glasses. The local viscoelastic moduli for both gels and glasses cross over from a single power law to the sum of two power laws around a certain time t_0. These results demonstrate the existence of two distinct contributions in the viscoelasticity of the system in the later stages of aging. In addition to a strongly frequency-dependent viscoelastic shear modulus at high frequencies $\cong \omega^{0.7}$, we also observe the slow development of a more elastic (only weakly frequency-dependent) shear modulus during the aging. The exponents of the power laws follow exactly the same time course of evolution for different concentrations if we scale the aging time as $t'_a = (t_a - t_0)/t_0$. This result is independent of the sample being a gel or a glass.

The crossover from a single frequency-dependent component to a superposition of a strongly frequency-dependent viscoelastic component plus a weakly frequency-dependent (elastic) component was previously interpreted in the context of polymer networks as being due to large inhomogeneities [30,31]. Here the sum of two power laws describes both gel (heterogenous) and glass (homogenous) local shear moduli, suggesting that locally the underlying physical process responsible for the evolution of gels and glasses is similar. This poses the rather puzzling question what is the physical origin of the two power laws in the viscoelasticity.

ACKNOWLEDGMENTS

[1] P. Sollich, F. Lequeux, P. Hebraud, and M. E. Cates Phys. Rev. Lett. **78**, 2020 (1997); S. M. Fielding, P. Sollich, and M. E. Cates, J. Rheol. **44**, 323 (2000);

[2] P. N. Pusey and W. van Megen, Phys. Rev. Lett. **59**, 2083 (1987); W. van Megen, S. M. Underwood, and P. N. Pusey, *ibid.* **67**, 1586 (1991); K. N. Pham, S. U. Egelhaaf, P. N. Pusey, and W. C. K. Poon, Phys. Rev. E **69**, 011503 (2004).

[3] M. Kroon, G. H. Wegdam, and R. Sprik, Phys. Rev. E **54**, 6541 (1996).

[4] D. Bonn, H. Kellay, H. Tanaka, G. H. Wegdam, and J. Meunier, Langmuir **15**, 7534 (1999), D. Bonn, H. Tanaka, H. Kellay, G. H. Wegdam, and J. Meunier, Europhys. Lett. **45**, 52 (1998).

[5] D. A. Weitz, J. S. Huang, M. Y. Lin, and J. Sung, Phys. Rev. Lett. **54**, 1416 (1985); M. Carpineti and M. Giglio, *ibid.* **68**, 3327 (1992); L. Cipelletti, S. Manley, R. C. Ball, and D. A. Weitz, *ibid.* **84**, 2275 (2000).

[6] W. K. Kegel and A. van Blaaderen, Science **287**, 290 (2000).

[7] K. N. Pham, G. Petekidis, D. Vlassopoulos, S. U. Egelhaaf, P. N. Pusey, and W. C. K. Poon, Europhys. Lett. **75**, 624 (2006).

[8] S. Jabbari-Farouji, G. H. Wegdam, and D. Bonn, Phys. Rev. Lett. **99**, 065701 (2007).

[9] P. Mayer, H. Bissig, L. Berthier, L. Cipelletti, J. P. Garrahan, P. Sollich, and V. Trappe, Phys. Rev. Lett. **93**, 115701 (2004).

[10] S. Jabbari-Farouji, H. Tanaka, G. H. Wegdam, and D. Bonn, Phys. Rev. E (to be published).

[11] P. Levitz, E. Lecolier, A. Mourchid, A. Delville, and S. Lyonnard, Europhys. Lett. **49**, 672 (2000).

[12] B. Ruzicka, L. Zulian, and G. Ruocco, Phys. Rev. Lett. **93**, 258301 (2004); Langmuir **22**, 1106 (2006).

[13] D. Bonn, P. Coussot, H. T. Huynh, F. Bertrand, and G. Debregeas, Europhys. Lett. **59**, 786 (2002).

[14] M. Bellour, A. Knaebel, J. L. Harden, F. Lequeux, and J.-P. Munch, Phys. Rev. E **67**, 031405 (2003); S. Kaloun, R. Skouri, M. Skouri, J. P. Munch, and F. Schosseler, *ibid.* **72**, 011403 (2005).

[15] F. Gittes, B. Schnurr, P. D. Olmsted, F. C. MacKintosh, and C. F. Schmidt, Phys. Rev. Lett. **79**, 3286 (1997); B. Schnurr, F. Gittes, F. C. MacKintosh, and C. F. Schmidt, Macromolecules **30**, 7781 (1997).

[16] M. Atakhorrami, K. M. Addas, and C. Schmidt, Rev. Sci. Instrum. **79**, 043103 (2008).

[17] M. Atakhorrami, J. I. Sulkowska, K. M. Addas, G. H. Koenderink, J. X. Tang, A. J. Levine, F. C. MacKintosh, and C. F. Schmidt, Phys. Rev. E **73**, 061501 (2006).

[18] T. Nicolai and S. Cocard, Langmuir **16**, 8189 (2000).

[19] A gift from Van't Hoff Laboratory, Utrecht University.

[20] M. Atakhorrami, Ph.D. thesis, Vrije Universiteit Amsterdam, 2006.

[21] F. Gittes and C. F. Schmidt, Methods Cell Biol. **55**, 129 (1998).

[22] F. C. MacKintosh and C. F. Schmidt, Curr. Opin. Colloid Interface Sci. **4**, 300 (1999).

[23] S. Jabbari-Farouji, D. Mizuno, M. Atakhorrami, F. C. MacKintosh, C. F. Schmidt, E. Eiser, G. H. Wegdam, and D. Bonn, Phys. Rev. Lett. **98**, 108302 (2007). S. Jabbari-Farouji, D. Mizuno, D. Denks, G. H. Wegdam, F. C. MacKintosh, C. F. Schmidt, and D. Bonn, Europhys. Lett. **84**, 20006 (2008).

[24] T. G. Mason and D. A. Weitz, Phys. Rev. Lett. **74**, 1250 (1995); T. G. Mason, H. Gang, and D. A. Weitz, J. Opt. Soc. Am. A **14**, 139 (1997).

[25] M. Buchanan, M. Atakhorrami, J. F. Palierne, F. C. MacKintosh, and C. F. Schmidt, Phys. Rev. E **72**, 011504 (2005); M. Atakhorrami and C. F. Schmidt, Rheol. Acta **45**, 449 (2006).

[26] K. M. Addas, C. F. Schmidt, and J. X. Tang, Phys. Rev. E **70**, 021503 (2004).

[27] A. J. Levine and T. C. Lubensky, Phys. Rev. E **65**, 011501 (2001).

[28] S. Jabbari-Farouji, Ph.D. thesis, University of Amsterdam, 2007.

[29] V. Trappe and D. A. Weitz, Phys. Rev. Lett. **85**, 449 (2000).

[30] M. L. Gardel, J. H. Shin, F. C. MacKintosh, L. Mahadevan, P. A. Matsudaira, and D. A. Weitz, Phys. Rev. Lett. **93**, 188102 (2004).

[31] F. Brochard and P. G. de Gennes, Macromolecules **10**, 1157 (1977); S. T. Milner, Phys. Rev. E **48**, 3674 (1993).